



The structure of $\text{As}_3\text{Se}_5\text{Te}_2$ infrared optical glass

P. Jóvári^{a,*}, B. Bureau^b, I. Kaban^c, V. Nazabal^b, B. Beuneu^d, U. Rütt^e

^a Research Institute for Solid State Physics and Optics, H-1525 Budapest, POB 49, Hungary

^b Equipe Verres et Céramiques, Laboratoire Sciences Chimiques de Rennes UMR-CNRS 6226, Campus de Beaulieu, Université de Rennes 1, 35042 Rennes Cedex, France

^c Institut of Physics, Chemnitz University of Technology, D-09107 Chemnitz, Germany

^d Laboratoire Léon Brillouin, CEA-Saclay 91191 Gif sur Yvette Cedex, France

^e Hamburger Synchrotronstrahlungslabor HASYLAB am Deutschen Elektronen-Synchrotron DESY, Notkestrasse 85 D-22603 Hamburg, Germany

ARTICLE INFO

Article history:

Received 1 July 2009

Received in revised form 29 August 2009

Accepted 31 August 2009

Available online 8 September 2009

PACS:

63.50.Lm

61.05.c

61.05.fm

61.05.cj

Keywords:

Amorphous materials

Atomic scale structure

Neutron diffraction

X-ray diffraction

EXAFS

ABSTRACT

The structure of $\text{As}_3\text{Se}_5\text{Te}_2$ infrared optical glass was investigated by X-ray and neutron diffraction as well as extended X-ray absorption fine structure measurements at the As-, Se- and Te K-edges. The five datasets were modelled simultaneously by the reverse Monte Carlo simulation technique. Experimental data could be fitted satisfactorily by allowing As–Se, As–Te and Se–Te bonds only. It was revealed that the affinity of As is much higher to Se than to Te. The nearest As–Se distance is similar to that found in other vitreous As–Se based alloys, while the As–Te bond length is 0.02–0.04 Å shorter in $\text{As}_3\text{Se}_5\text{Te}_2$ than in binary As–Te glasses.

© 2009 Elsevier B.V. All rights reserved.

1. Introduction

As–Se–Te glasses are extensively used in optical fibres [1,2] in the mid-infrared region (2–12 μm). The composition $\text{As}_3\text{Se}_5\text{Te}_2$ proved to be especially promising due to its relatively low attenuation (0.5 dB/m between 6.5 μm and 9.5 μm). Besides its excellent optical properties, this alloy also possesses appropriate thermal stability and chemical resistance. The above favourable combination of properties makes it suitable for practical applications such as infrared sensors in chemistry [3,4], biology [5,6], medicine [7–9] or telecommunication and space optics [10–12]. Indeed, alloying the As–Se glasses with Te shifts the multi-phonon absorption to longer wavelengths and simultaneously increases the glass forming ability and resistivity against crystallization ($\text{As}_3\text{Se}_5\text{Te}_2$ shows no crystallization when heated at rates between 5 K/min and 20 K/min [13]).

Both Se and Te form binary glasses with As over a wide composition range. $\text{As}_x\text{Te}_{100-x}$ alloys can be vitrified for $20 \leq x \leq 60$ [14],

while As–Se glasses can be obtained from pure Se up to ~55 at.% As. In the As–Te system most physical properties (e.g. hardness, glass transition temperature) evolve monotonously with composition while non-monotonous composition dependence can be observed in As–Se glasses where the above properties reach the maximum at the stoichiometric composition (As_2Se_3). This discrepancy is caused by the entirely different bonding preferences governing the two systems. In As–Se glasses the prevailing factor is the minimization of the number of homonuclear bonds. There is no such tendency in the As–Te system where As–As and Te–Te bonding is significant over the whole glass forming region [15].

In spite of their potential applications, the structure of glassy As–Se–Te alloys has not yet received much attention. In the present study, we report the results of a detailed investigation on $\text{As}_3\text{Se}_5\text{Te}_2$ glass by X-ray and neutron diffraction as well as extended X-ray absorption (EXAFS) measurements at the As, Se and Te K-absorption edges. The five datasets were modelled by the reverse Monte Carlo simulation technique [16–18]. Resulting particle configurations were analysed in terms of nearest neighbour distances, coordination numbers and bond angle distributions. The results are compared with the short range order parameters of binary As–Te and As–Se glasses.

* Corresponding author. Tel.: +36 1 392 25 89; fax: +36 1 392 25 89.

E-mail address: jovari@sunserv.kfki.hu (P. Jóvári).

2. Experimental and modelling

2.1. Sample preparation

Raw materials of high purity (99.999%) were used for glass preparation, which is described in detail elsewhere [19,20]. Selenium and arsenic were purified of remaining oxygen and hydrogen with the volatilization technique by heating them, respectively at 240 °C and 290 °C under vacuum for several hours. As for tellurium, the oxide surface layer was dissolved in liquid HBr. After these treatments, the required amounts of Te, As and Se were sealed in a silica tube under vacuum and the mixture was distilled and then maintained at 700 °C for 12 h in a rocking furnace to ensure a good homogenization of the liquid. Then the ampoule was quenched in water. The glassy alloy obtained was annealed near the glass transition temperature (T_g) to remove mechanical stresses produced on cooling.

2.2. Measurements

The high energy X-ray diffraction measurement was carried out at the BW5 experimental station [21] of HASYLAB. Powdered sample was placed into a thin walled (20 µm) quartz capillary of 2 mm diameter. The energy of the radiation was 109.5 keV ($\lambda = 0.113$ Å). Raw data were corrected for background scattering, detector deadtime and variations in detector solid angle [22].

The neutron diffraction experiment was carried out at the 7C2 liquid and amorphous diffractometer (LLB, Saclay). Powder sample was filled into a thin walled vanadium can (5 mm diameter, 0.1 mm wall thickness). The wavelength was 0.72 Å. Raw intensities were corrected for empty instrument background, scattering from empty sample holder, multiple scattering [23], absorption [24] and detector efficiency.

As, Se and Te K-edge extended X-ray absorption fine structure (EXAFS) data were recorded at the beamline X1 of HASYLAB. Finely ground powder of $As_{30}Se_{50}Te_{20}$ was mixed with cellulose and pressed into tablets. The transmission of the tablets was about 1/e around the absorption edges. Intensities were recorded by ionization chambers filled with Ar/N₂ mixtures.

2.3. Simulation details

RMC [16–18] offers a framework for generating large scale structural models compatible with experimental data (diffraction and EXAFS). Available structural information can also be incorporated into the models in the form of minimum interatomic distances (cut offs), coordination number and bond angle constraints. The usage of constraints makes it possible to test structural hypotheses in a rather straightforward manner. This way it was shown, for example, that the experimental data on amorphous $Ge_2Sb_7Te_5$ cannot be interpreted without Sb–Ge and Ge–Ge bonds [25,26]. It should be noted that there is no other simple scheme that can directly combine diffraction and EXAFS measurements either in real or reciprocal space. For details of the simultaneous fitting of diffraction and EXAFS datasets and the use of coordination constraints, we refer to some recent papers [15,18].

In the present work, simulation boxes contained 12,000 atoms. The density of atoms in the simulation box was 0.0332 Å⁻³. This value was obtained by interpolating the number densities of $As_{30}Se_{70}$ and $As_{30}Te_{70}$ [14].

3. Results and discussion

To check which types of bonds are present in the glassy $As_3Se_5Te_2$, several test runs were carried out with different cut off distances. Finally, it was found that only As–Se, As–Te and Te–Se bonds are needed to get reasonable fits and reasonable coordination numbers ($N_{As} \approx 3$, $N_{Se} \approx 2$ and $N_{Te} \approx 2$). Threefold coordination of As and twofold coordination of Se are in agreement with NMR data collected from As_xSe_{1-x} glasses [27]. Moreover, allowing other types of bonds (by lowering the corresponding minimum interatomic distances in the model below the covalent bond length) did not improve the quality of fits but often resulted in an artificial ‘crosstalk’ between different pair correlations. For example, when Se–Se bonding was also allowed, N_{Se} increased to about 2.4 and N_{As} decreased to about 2.3. The reason for this is that As and Se possess rather similar X-ray and photoelectron scattering power due to their close electron numbers. The difference of their neutron scattering lengths is also moderate ($b_{As} = 6.58$ fm, $b_{Se} = 7.97$ fm [28]), which makes it hardly possible to distinguish between them. As a result, RMC produces configurations in which As and Se are mixed in a completely random way. This information deficiency can be overcome only by applying an additional constraint in the simulation. In the present case, it was achieved by increasing the minimum

Table 1

Cut off distances obtained by test simulation runs.

Type of pairs	Te–Te	Te–As	Te–Se	As–As	As–Se	Se–Se
Cut off [Å]	3.1	2.4	2.4	3.1	2.1	3.0

Se–Se distance from 2.1 Å to 3 Å. As it could be done without any worsening of the fits, and the resulting coordination numbers agree very well with the 8-*N* rule [29], it is reasonable to assume that our model is realistic. We mention here that models compatible with the 8-*N* rule could also be obtained by allowing Te–Te bonding. However, as the number of Te–Te pairs in the test RMC simulation runs was rather low ($N_{TeTe} \approx 0.4$) and the fits were not improved, they have not been considered further.

Minimum interatomic distances used in the simulation allowing only As–Se, As–Te and Te–Se bonds are listed in Table 1. Fits and partial pair correlation functions obtained by the simulation run are shown in Figs. 1 and 2, while the coordination numbers and bond lengths are summarized in Table 2. The N_{ij} coordination numbers (the average numbers of *j* type atoms around an *i* type atom) are defined by the following equation:

$$N_{ij} = 4\pi\rho c_j \int_0^R g_{ij}(r)r^2 dr \quad (1)$$

Here ρ is the number density, c_j is the concentration of *j* type atoms, and R is the upper limit of the coordination sphere, which is in each case the minimum of the corresponding partial pair correlation function. N_i , the average total number of neighbours of type *i* atoms is given simply by the following sum:

$$N_i = \sum_j N_{ij} \quad (2)$$

While the presence of As–Se and Te–Se bonds is rather trivial, the lack of As–As bonds does not necessarily follow from the simple chemical considerations. It was shown, for example, that As–As bonds exist in As–Te glasses even at 20 at.% As concentration,

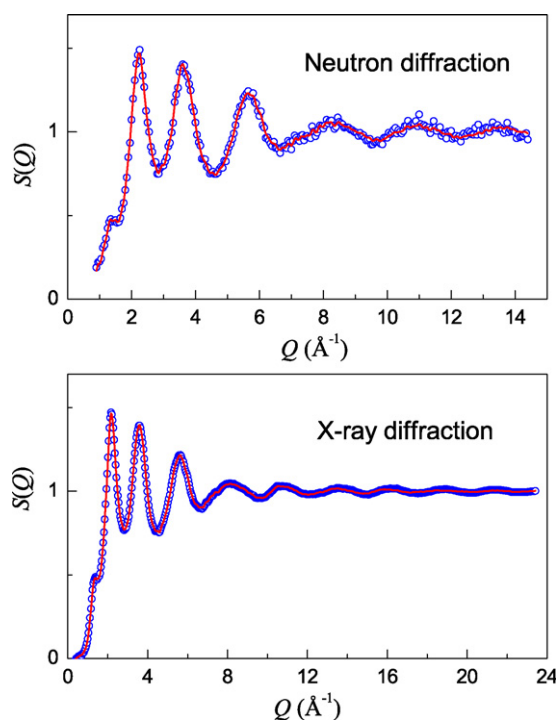


Fig. 1. Fit of neutron- and X-ray diffraction data obtained by simultaneous fit of the five experimental datasets.

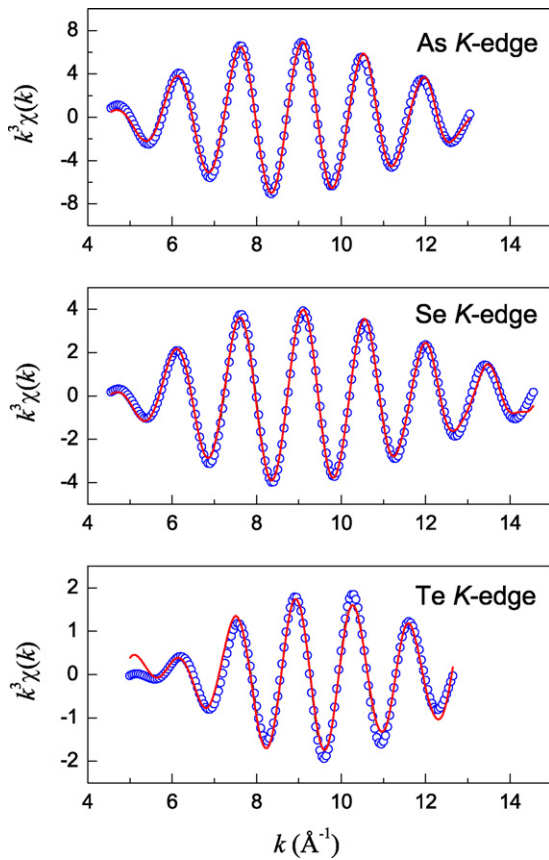


Fig. 2. Fit of the three EXAFS datasets obtained by simultaneous fit of the five experimental datasets.

where the As–As coordination number N_{AsAs} is as high as 1.05 ± 0.2 [15].

Comparison of the ratio of Se and Te concentrations ($0.5/0.2 = 2.5$) and the ratio of N_{AsSe} and N_{AsTe} ($2.57/0.53 \approx 4.8$) reveals that Te and As tend to avoid each other.

The As–Se distance obtained in the present work is 2.41 \AA . This value agrees well with the findings of some experimental studies on binary As–Se glasses ($2.40\text{--}2.43 \text{ \AA}$) [30–32]. The As–Te bond length is $2.55 \pm 0.02 \text{ \AA}$, which is somewhat shorter than the As–Te distance in binary As_xTe_{100-x} alloys ($2.58\text{--}2.59 \text{ \AA}$ for $x \geq 34$) [15]. On the other hand, Se–Te bond length is 2.60 \AA , which is longer than the mean Se–Te distance observed in binary Se–Te glasses ($2.54\text{--}2.56 \text{ \AA}$) [33,34].

It is to be emphasized that the average coordination numbers of As, Se and Te were obtained without applying coordination constraints. Thus N_{As} , N_{Se} and N_{Te} are determined by the experimental data and the minimum interatomic distances. Their small deviation from the 8- N values (3, 2 and 2, respectively) suggests that in the present case the error of N_i coordination numbers is in the order of a few percent.

In general the uncertainty of N_{ij} coordination numbers extracted from an atomic configuration generated by RMC can be estimated by additional simulation runs. In these runs N_i values are fixed as constraints and the system is perturbed by forcing a selected k - l

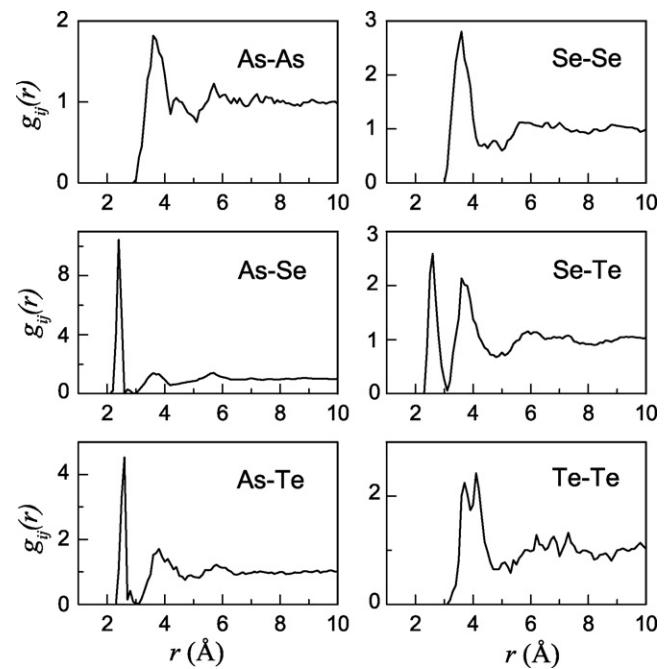


Fig. 3. Partial pair correlation functions obtained by the simultaneous modelling of the five measurements (only As–Se, As–Te and Se–Te bonds were allowed).

coordination number to deviate from its initial value by δN_{kl} . The response to the perturbation is usually twofold: (i) some N_{ij} values change to satisfy the constraint imposed on N_i coordination numbers; (ii) some fits start to get worse or some unphysical features appear on one or more partial pair correlation functions. Then δN_{kl} can be considered as the uncertainty of N_{kl} . A similar procedure was applied in [35] to estimate the error of some coordination numbers in $Co_{43}Fe_{20}Ta_{5.5}B_{31.5}$ metallic glass.

The above scheme can be used if the number of free N_{ij} values is greater than the number of fixed N_i coordination numbers. This condition is satisfied for most multicomponent alloys. In our case, however, satisfactory fits and partial pair correlation functions can be obtained by allowing only three types of bonds (As–Se, As–Te, Se–Te). Thus only N_{AsSe} , N_{AsTe} and N_{SeTe} differ from zero. N_{SeAs} , N_{TeAs} and N_{TeSe} can be obtained from these by the following relation:

$$N_{ji} = \frac{c_j}{c_i} N_{ij} \quad (3)$$

If we assume that $N_{As} = 3$, $N_{Se} = 2$ and $N_{Te} = 2$ then N_{AsSe} , N_{AsTe} and N_{SeTe} are already uniquely determined and can be obtained from N_{As} , N_{Se} and N_{Te} by simple linear algebraic manipulations. These values are compared with the results of our unconstrained simulation run in Table 2. The excellent overall agreement suggests that our basic assumptions – (i) the 8- N rule is obeyed; (ii) there are only As–Se, As–Te and Se–Te bonds in the alloy – are satisfied by the majority of atoms. In principle, there is no reason to believe that in the present case the uncertainty of N_{ij} values is much higher than that of N_i coordination numbers. Therefore, the double of the maximum deviation from the 8- N rule ($2 \times 0.1 = 0.2$) can be regarded as a conservative estimate of the uncertainty of N_{ij} values.

Table 2

Coordination numbers (N_i and N_{ij}) and nearest neighbour distances (r_{ij} , in \AA) obtained by unconstrained RMC simulation. Values in bold have been determined by assuming that each atom satisfies the 8- N rule and there are only As–Se, As–Te and Se–Te bonds. The uncertainty of r_{ij} values is about $\pm 0.02 \text{ \AA}$.

N_{Te}	N_{As}	N_{Se}	N_{TeAs}	N_{TeSe}	N_{AsSe}	N_{AsTe}	N_{SeTe}	N_{SeAs}	r_{TeAs}	r_{TeSe}	r_{AsSe}
2.01	3.10	2.03	0.79	1.22	2.57	0.53	0.49	1.54	2.56	2.60	2.41
2	3	2	0.75	1.25	2.5	0.5	0.5	1.5	–	–	–

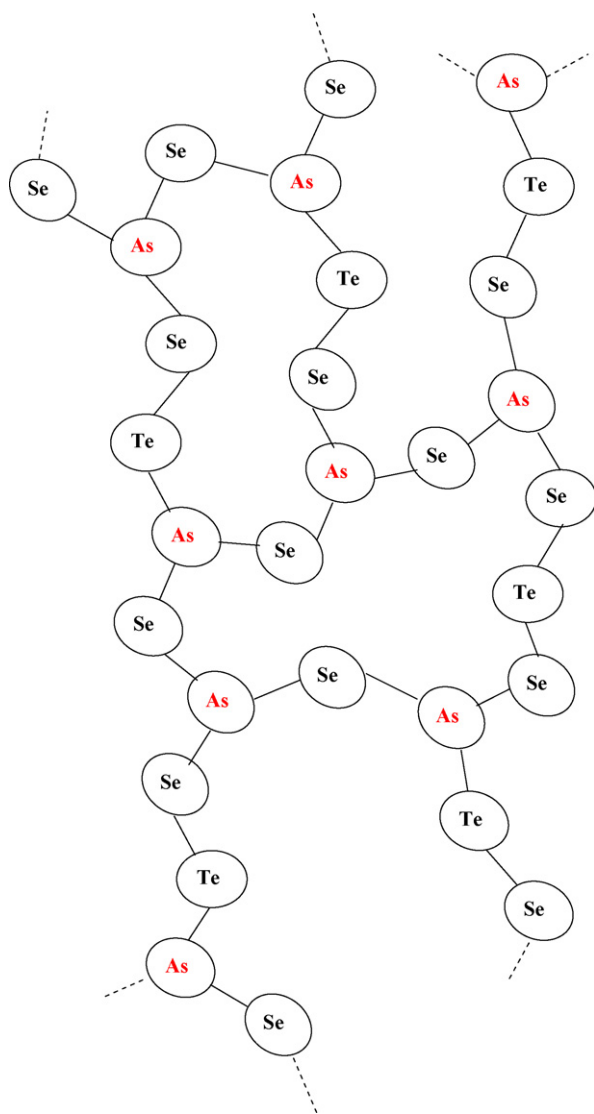


Fig. 4. A schematic network structure accounting for all bonding preferences in glassy $\text{Te}_2\text{As}_3\text{Se}_5$.

The absence of Te–Te bonds means that on a microscopic scale Te atoms are distributed homogeneously over the network. Both As–As and Se–Se partial pair distribution functions have the first peak around 3.7 Å corresponding to the second neighbour As–As and Se–Se distances. The mean Se–As–Se angle is equal to 101°. The second neighbour distance is shifted to about 4 Å when tellurium atoms are embedded in the network (Fig. 3). This distance is also in agreement with Te–As–Te angle equal to about 100°.

A schematic model accounting for all the above findings is shown in Fig. 4. The lone pairs (two for Se/Te, one for As) are not represented. This network scheme possesses the proper stoichiometry and can be viewed as such sequences connected to each other. The basic units are $\text{As}(\text{Se}, \text{Te})_3$ pyramids connected directly or via chalcogene atoms. Note that in the first situation the bridging chalcogene is rather Se than Te considering the higher affinity of As to Se. This structural model explains the higher glass transition temperature compared to the glasses strictly based on Se and Te. Moreover, this sketch shows that Te atoms have to be well diluted into the network to agree the above structural findings. These results are in fair agreement with NMR studies of Se–Te glasses, which have shown that Se and Te atoms are almost perfectly randomly distributed [36]. It is also very coherent with the physical

properties of that technical glass. First, its optical transmission is larger in the mid-infrared than for equivalent As–Se glasses due to the larger mass of tellurium atoms spreading homogeneously over the network. Second, $\text{As}_3\text{Se}_5\text{Te}_2$ present no crystallisation peaks. Indeed, it is well known that in glasses containing tellurium, microcrystals originate from short sequences of Te atoms which play the role of nucleating agent [2].

4. Conclusions

The structure of glassy $\text{As}_3\text{Se}_5\text{Te}_2$ was investigated by fitting simultaneously five experimental datasets by the reverse Monte Carlo simulation technique. Good fits could be obtained by allowing As–Se, As–Te and Se–Te bonds only. It was found that all atoms satisfy the 8–N rule ($N_{\text{As}} = 3$, $N_{\text{Se}} = N_{\text{Te}} = 2$ within experimental uncertainties). It was also revealed that the affinity of As is much higher to Se than to Te. Chalcogenide atoms bond preferentially to As, and Se–Te bonds are formed only after saturating all valences of As. The nearest As–Se distance is similar to that found in other vitreous As–Se based alloys, while the Te–As bond length in $\text{As}_3\text{Se}_5\text{Te}_2$ glass is 0.02–0.04 Å shorter than in binary As–Te glasses. Finally, the simulation leads to a glass network built up of $\text{As}(\text{Se}, \text{Te})_3$ pyramids in which Te atoms homogeneously substitute Se in good agreement with the thermal and optical properties of this technical glass for infrared application.

Acknowledgements

P. Jóvári was supported by the Bolyai Research Fellowship of the Hungarian Academy of Sciences and by the Hungarian Basic Research Found (OTKA) grant no. T048580. I. Kaban acknowledges DESY for the financial support. Fruitful discussions with John C. Mauro (Corning Inc.) are greatly acknowledged. The neutron diffraction measurement at Saclay (France) was supported by the European Commission under the 6th Framework Programme through the Key Action: Strengthening the European Research Area, Research Infrastructures. Contract No.: HIII-CT-2003-505925.

References

- [1] X.H. Zhang, B. Bureau, C. Boussard, H.L. Ma, J. Lucas, *Chemistry* 14 (2008) 432–442.
- [2] B. Bureau, S. Danto, H.L. Ma, C. Boussard-Plédel, X.H. Zhang, J. Lucas, *Solid State Sci.* 10 (2008) 427–433.
- [3] D. Le Coq, K. Michel, J. Keirsse, C. Boussard-Plédel, G. Fonteneau, B. Bureau, J.M. Le Quéré, O. Sire, J. Lucas, *C. R. Chim.* 5 (2003) 1–7.
- [4] D. Le Coq, C. Boussard-Plédel, G. Fonteneau, T. Pain, B. Bureau, J.L. Adam, *Mater. Res. Bull.* 38 (13) (2003) 1745–1754.
- [5] J. Keirsse, C. Boussard-Plédel, O. Loréal, O. Sire, B. Bureau, B. Turlin, P. Leroyer, J. Lucas, *J. Non-Cryst. Solids* 327 (2003) 430–433.
- [6] P. Lucas, M. Riley, C. Boussard, B. Bureau, *Anal. Biochem.* 351 (2006) 1–10.
- [7] J. Keirsse, C. Boussard-Plédel, O. Loréal, O. Sire, B. Bureau, P. Leroyer, B. Turlin, J. Lucas, *Vib. Spectrosc.* 32 (2003) 23–32.
- [8] S. Hocdé, O. Loréal, O. Sire, C. Boussard-Plédel, B. Bureau, B. Turlin, J. Keirsse, P. Leroyer, J. Lucas, *J. Biomed. Opt.* 9 (2004) 404–407.
- [9] P. Lucas, M. Solis, D. LeCoq, C. Junker, M. Riley, J. Collier, D. Boesewetter, C. Boussard, B. Bureau, *Sens. Actuator B* 119 (2006) 355–362.
- [10] W. Shen, M. Cathelinaud, M. Lequime, V. Nazabal, X. Liu, *Opt. Commun.* 281 (2008) 3726–3731.
- [11] P. Houizot, C. Boussard-Plédel, A.J. Faber, L. Cheng, B. Bureau, P.A. Nijnatten, W. Gielesens, J. Pereira, J. Lucas, *Opt. Express* 15 (2007) 12529–12538.
- [12] A. Wilhelm, C. Boussard, Q. Coulombier, J. Lucas, B. Bureau, P. Lucas, *Adv. Mater.* 19 (2007) 3796–3800.
- [13] V.S. Shiryaev, J.-L. Adam, X.H. Zhang, C. Boussard-Plédel, J. Lucas, M.F. Churbanov, *J. Non-Cryst. Solids* 336 (2004) 113–119.
- [14] Z.U. Borisova, *Glassy Semiconductors*, Plenum, New York, 1981.
- [15] P. Jóvári, S.N. Yannopoulos, I. Kaban, A. Kalampounias, I. Lishchynskyy, B. Beuneu, O. Kostadinova, E. Welter, A. Schöps, *J. Chem. Phys.* 129 (2008) 214502.
- [16] L. Pusztai, R.L. McGreevy, *Phys. B* 234–236 (1997) 357–358.
- [17] R.L. McGreevy, *J. Phys.: Condens. Matter* 13 (2001) R877–R913.
- [18] O. Gereben, P. Jóvári, L. Temleitner, L. Pusztai, *J. Optoelectron. Adv. Mater.* 9 (2007) 3021–3027.

- [19] X.H. Zhang, H.L. Ma, C. Blanchetière, J. Lucas, J. Non-Cryst. Solids 161 (1993) 327–330.
- [20] S. Hocdé, C. Boussard-Plédel, G. Fonteneau, D. Le Coq, H.L. Ma, J. Lucas, J. Non-Cryst. Solids 274 (2000) 17–22.
- [21] R. Bouchard, D. Hupfeld, T. Lippmann, J. Neuefeind, H.-B. Neumann, H.F. Poulsen, U. Rütt, T. Schmidt, J.R. Schneider, J. Süßenbach, M. von Zimmermann, J. Synchrotron Radiat. 5 (1998) 90–101.
- [22] H.F. Poulsen, H.-B. Neumann, J.R. Schneider, J. Neuefeind, M.D. Zeidler, J. Non-Cryst. Solids 188 (1995) 63–74.
- [23] I.A. Blech, B.L. Averbach, Phys. Rev. 137 (1965) A1113–A1116.
- [24] H.H. Paalman, J.C. Pings, J. Appl. Phys. 33 (1962) 2635–2639.
- [25] P. Jóvári, I. Kaban, J. Steiner, B. Beuneu, A. Schöps, A. Webb, J. Phys.: Condens. Matter 19 (2007) 335212.
- [26] P. Jóvári, I. Kaban, J. Steiner, B. Beuneu, A. Schöps, A. Webb, Phys. Rev. B 77 (2008) 035202.
- [27] B. Bureau, J. Troles, M. Le Floch, F. Smektala, G. Silly, J. Lucas, Solid State Sci. 5 (2003) 219–224.
- [28] V.F. Sears, Neutron News 3 (3) (1992) 26–37.
- [29] N. Mott, Adv. Phys. 16 (1967) 49–144.
- [30] T. Petkova, P. Petkov, P. Jóvári, I. Kaban, W. Hoyer, A. Schöps, A. Webb, B. Beuneu, J. Non-Cryst. Solids 353 (2007) 2045–2051.
- [31] S. Hosokawa, Y. Wang, W.-C. Pilgrim, J.-F. Bézar, S. Mamedov, P. Boolchand, J. Non-Cryst. Solids 352 (2006) 1517–1519.
- [32] Y. Iwadate, T. Hattori, S. Nishiyama, K. Fukushima, Y. Mochizuki, M. Misawa, T. Fukunaga, J. Phys. Chem. Solids 60 (1999) 1447–1451.
- [33] M. Majid, S. Bénazeth, C. Souleau, J. Purans, Phys. Rev. B 58 (1998) 6104–6114.
- [34] K. Itoh, M. Misawa, T. Fukunaga, J. Non-Cryst. Solids 293–295 (2001) 575–579.
- [35] I. Kaban, P. Jóvári, M. Stoica, J. Eckert, W. Hoyer, B. Beuneu, Phys. Rev. B 79 (2009) 212201.
- [36] B. Bureau, C. Boussard-Plédel, J. Troles, M. Le Floch, F. Smektala, J. Lucas, J. Phys. Chem. B 109 (2005) 6130–6135.